

# Surface Morphology and Chemically Active Sites on Ru Based Ultracapacitors: Montecarlo Simulation with Embedded Atom Potentials

Lesser Blum, Marc D Legault, Fredy R Zypman

University of Puerto Rico

l\_blum@uprac.upr.clu.edu

marc@web.uprr.pr

f\_zypman@cuhac.upr.clu.edu

## ABSTRACT

Transition metals and their oxides play an important role as catalyzers in chemical reactions occurring in modern batteries. In particular, ruthenium (Ru) has been identified as a promising candidate for use in next-generation batteries for electrical vehicle applications. An understanding of ruthenium's surface morphology in relation to its chemically active sites will clarify its use in these batteries and help optimize their design. A first-step in this understanding is achieved by providing means to calculate surface energies and investigate surface reconstructions within the framework of the Embedded Atom Method (EAM). The parameters that define the embedding function  $\mathcal{F}$  and the pair potential  $\Phi$  for Ru are adjusted such that the elastic constants calculated from the EAM expressions reproduce experimentally known data. A Monte-Carlo Simulated Annealing algorithm is used for the fitting process. These best-fit parameters are then used to calculate the Ru surface energy.

Keywords: Ultracapacitors, batteries, catalysis, EAM.

## INTRODUCTION

Ultracapacitors are electrochemical energy storage devices with characteristics of both the classical dielectric capacitor and the electrochemical battery. A detailed comparison of these energy storage systems is given by Conway [1]. Ultracapacitors can store large amounts of energy like a battery and can also release that energy quickly like a capacitor. This characteristic makes the ultracapacitor a high-storage and high-power device which is ideal for use in electrical vehicles. The most important electrochemical reactions in ultracapacitors occur at the surface of solid ruthenium or ruthenium oxide in contact with a sulfuric acid electrolyte[2,3]. A complete understanding of the processes that take place at the ruthenium or ruthenium oxide surface necessarily involves an understanding of the structure and dynamics of the inner layer (the monolayer adjacent to the electrode surface) and also the diffuse layer (layer of solution just a few nanometers thick near the electrode surface). Electrolyte atoms of the inner layer may: chemisorb on the metal surface by chemically bonding to the metal (or oxide) atoms, move freely on the surface, or they

may react with surface atoms and then move away from the surface to form one of the end-products of the electrochemical reaction.

An experimental study of these reactions occurring at the surface is difficult to perform due to intrinsic measurement technique limitations. These reactions occur mainly on a two-dimensional surface and most traditional methods of investigation cannot be used. However, surface analytical techniques like EXAFS, NEXAFS, LEED, HREEL, STM and SFM have been developed to minimize this problem. Experimental data is also difficult to interpret because the metal surface is not homogeneous. Microscopic models of the metal-electrolyte system are required to interpret the raw experimental data.

Many transition metals have been theoretically studied using first-principles and semi-empirical quantum mechanical methods[4]. However since ruthenium has not been studied extensively we propose as a first-step to study the ruthenium surface without the electrolyte.

## BACKGROUND

Most metal surfaces undergo relatively large scale reconstructions which prohibit *ab initio* quantum mechanical energy calculations due to the large amount of atoms in the system. It is possible to calculate the energy directly with phenomenological pair-potential approaches, however they incorrectly treat the elastic properties, cohesive energy, and other many-body effects in solids. Many-body semi-empirical methods are widely used to calculate ground-state properties of real materials[5].

The Embedded Atom Method (EAM)[6] is computationally fast and widely used for semi-empirical quantum mechanical calculations on large and complex realistic metallic systems. This method has been successfully applied to bulk and interface problems[7]. It presents an appealing physical picture of a microscopic metallic system. Each atom of the metal is viewed as an impurity embedded in a host of all other atoms in the metal. The embedding energy is defined as the energy obtained by immersing an atom in the local

electron density created by its neighboring atoms.

In the EAM the total energy of a collection of atoms is the sum of individual atomic contributions  $i$ , where each contribution is the sum of the embedding energy  $\mathcal{F}_i(\rho_i)$  of an atom at site  $i$ , and a repulsive core-core energy  $\sum_j \Phi_i(R_{ij})$  produced by the interaction of atom  $i$  with all other atoms  $j$  in the system.  $\rho_i$  is the total electronic density evaluated at site  $i$  and  $R_{ij}$  is the distance between atoms  $i$  and  $j$ . The total energy of the system is then

$$E_{total} = \sum_i \mathcal{F}_i(\rho_i) + \frac{1}{2} \sum_{i,j} \Phi_{ij}(R_{ij}) \quad (1)$$

The embedding energy functional  $\mathcal{F}_i(\rho_i)$  incorporates many-body interactions to describe metallic bonding. The host electron density  $\rho_i$  is written as a linear superposition of atomic densities which are calculated using Roothan-Hartree-Fock self-consistent field theory. In this investigation we parametrize the functions  $\mathcal{F}$  and  $\Phi$  in the standard fashion, which we describe in the next section.

## EAM FUNCTIONS

To obtain  $\mathcal{F}_i(\rho_i)$  and  $\Phi_{ij}(R)$  for our system we first parametrize[8] the pair potential  $\Phi$  as

$$\Phi_{ij}(R) = \frac{Z_i(R)Z_j(R)}{R}, \quad (2)$$

with

$$Z_i(R) = Z_o(1 + \beta R)e^{-\alpha R}. \quad (3)$$

$Z_o$  is the charge of the valence electrons and  $Z_i$  is an effective screened charge.  $\alpha$  and  $\beta$  are fitting parameters. The typical behavior of  $Z(R)$  is shown in Fig. 1.

The embedding function  $\mathcal{F}(\rho)$  should satisfy the following conditions[6]:

- it has a single minimum,
- it is linear in  $\rho$  at high densities,
- it vanishes at zero density,
- its second derivative vanishes at zero density,
- and its second derivative must be negligible when  $\mathcal{F} = 0$ .

The above conditions are satisfied by the following embedding function

$$\mathcal{F}(\rho) = K_o\rho - a\rho e^{-b\rho^2} \quad (4)$$

where  $K_o$ ,  $a$ , and  $b$  are fitting parameters. Figure 2 shows the general shape of the embedding function  $\mathcal{F}(\rho)$ .

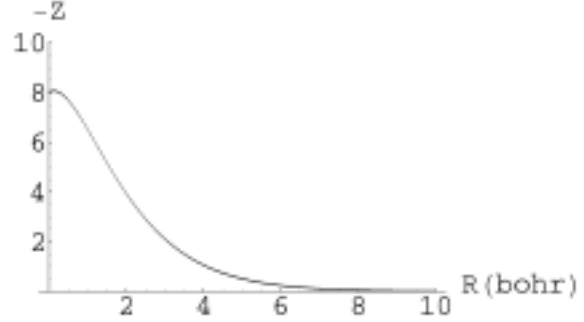


Fig. 1. Screened charge vs separation between two atoms.

For ruthenium the valence electron charge  $Z_o$  is eight and the five fitting parameters  $\alpha$ ,  $\beta$ ,  $K_o$ ,  $a$ , and  $b$  are adjusted such that the five independent elastic constants and sublimation energy as calculated using EAM reproduce their experimentally known values[9]. As described in reference [6], the elastic constants in terms of the EAM functions  $\mathcal{F}$  and  $\Phi$  are obtained using

$$C_{ijkl} = \frac{1}{\Omega_o} [B_{ijkl} + W_{ijkl}\mathcal{F}'(\rho_{eq}) + V_{ij}V_{kl}\mathcal{F}''(\rho_{eq})] \quad (5)$$

where

$$B_{ijkl} = \frac{1}{2} \sum_m (\Phi''_m - \frac{\Phi'_m}{a^m}) \frac{a^m_i a^m_j a^m_k a^m_l}{(a^m)^2}, \quad (6)$$

$$W_{ijkl} = \frac{1}{2} \sum_m (\rho''_m - \frac{\rho'_m}{a^m}) \frac{a^m_i a^m_j a^m_k a^m_l}{(a^m)^2}, \quad (7)$$

and

$$V_{ij} = \sum_m \frac{\rho'_m a^m_i a^m_j}{a^m}. \quad (8)$$

$\Omega_o$  is the unrelaxed atomic volume and for ruthenium is equal to 91.523 bohr<sup>3</sup>. The  $a^m_i$  are the  $i = x, y, z$  components of

$$\vec{a}^m = \sum_{i=x,y,z} a^m_i \hat{x}_i \quad (9)$$

where the indices  $m$  tag all atomic sites with positions

$$\vec{r}_{KLM} = a(K - \frac{L}{2})\hat{x} + aL\frac{\sqrt{3}}{2}\hat{y} + Mc\hat{z} \quad (10)$$

and

$$\vec{r}'_{KLM} = \vec{r}_{KLM} + \frac{a}{2}\hat{x} + \frac{a}{2\sqrt{3}}\hat{y} + \frac{c}{2}\hat{z} \quad (11)$$



Fig. 2. Embedding function vs electronic density as explained in the text.

where  $K$ ,  $L$ , and  $M$  are integers. The values of  $\rho_m$  and  $\Phi_m$  and their derivatives are evaluated at equilibrium.

Ruthenium crystallizes in a hexagonal closed packed configuration with lattice parameter  $a = 5.1117$  bohr and  $c = 8.0892$  bohr[10]. The spherically averaged electron density  $\rho(R)$  (see Fig. 3) is obtained from first principles Roothan-Hartree-Fock self-consistent field solution of the Schrödinger equation[11].

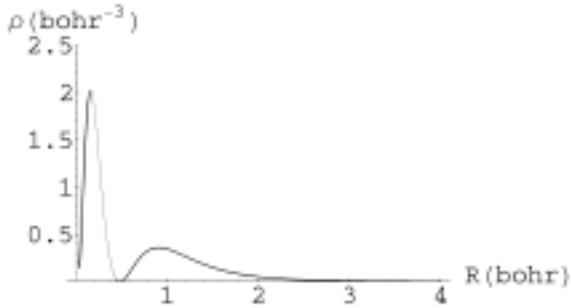


Fig. 3. Electronic density vs radial distance measured from the center of an atom. This was obtained from Roothan-Hartree-Fock self-consistent field solution to Schrödinger's equation.

Using the lattice parameters and  $\rho(R)$  for Ru and considering only the first- and second-nearest neighbors,

Eq. (5) generates the following five independent elastic constant equations

$$C_{11} = 49.42\xi^2 e^{-10.12\alpha} + 500.2\alpha\xi^2 e^{-10.12\alpha} + 1687\alpha^2\xi^2 e^{-10.12\alpha} - 0.06019d + 0.06019K_o + 9.507 \times 10^{-6}bd - 1.227 \times 10^{-10}b^2d, \quad (12)$$

$$C_{12} = 16.47\xi^2 e^{-10.12\alpha} + 166.7\alpha\xi^2 e^{-10.12\alpha} + 562.5\alpha^2\xi^2 e^{-10.12\alpha} - 0.02006d + 0.02006K_o + 6.777 \times 10^{-6}bd - 1.227 \times 10^{-10}b^2d, \quad (13)$$

$$C_{13} = 12.37\xi^2 e^{-10.12\alpha} + 125.3\alpha\xi^2 e^{-10.12\alpha} + 422.6\alpha^2\xi^2 e^{-10.12\alpha} - 0.01507d + 0.01507K_o + 6.1088 \times 10^{-6}bd - 1.1525 \times 10^{-10}b^2d, \quad (14)$$

$$C_{33} = 46.49\xi^2 e^{-10.12\alpha} + 470.5\alpha\xi^2 e^{-10.12\alpha} + 1587\alpha^2\xi^2 e^{-10.12\alpha} - 0.05662d + 0.05662K_o + 8.62 \times 10^{-6}bd - 1.082 \times 10^{-10}b^2d, \quad (15)$$

$$C_{55} = 12.38\xi^2 e^{-10.12\alpha} + 125.27\alpha\xi^2 e^{-10.12\alpha} + 422.6\alpha^2\xi^2 e^{-10.12\alpha} - 0.01507d + 0.01507K_o + 1.02528 \times 10^{-6}bd. \quad (16)$$

The parameter  $d$  in the above equations is in term of the fitting parameters  $a$  and  $b$  and is defined by  $d = ae^{-0.000034b}$  and also  $\xi$  is defined as  $\xi = (1 + 5.06042\beta)^2$ . In addition to the elastic constants expressions we include an expression for the sublimation energy

$$E_s = 0.005832d - 0.005832K_o - 75.88\xi^2 e^{-10.12\alpha}. \quad (17)$$

These nonlinear equations function of the EAM fitting parameters are solved using the Simulated Annealing Montecarlo algorithm of Metropolis [12]. A typical annealing run is started at a "high" temperature of  $T_i = 1000$  K where the system of equations are equilibrated and cooled down to 0.1 K using the annealing schedule of  $T_f = 0.9999T_i$ . Our obtained best-fit parameters and corresponding fit between EAM calculated and experimental properties (in Mbar for the elastic constants and hartree for the sublimation energy) are shown in Table 1. Figures 1, 2, and 4 show the plots of the EAM functions calculated using these parameters.

## ACKNOWLEDGMENTS

This work has been supported with grants from the **National Science Foundation** (DMR #9872689) and the **Department of Energy** (DE-FG02-98-ER-45729 and Subcontract from UNM). MDL acknowledges the Colegio Universitario de Bayamón for release time.

## REFERENCES

- [1] BE Conway, "Electrochemical Science and Technology", J Electrochem Soc **138**, 1539 (1991)
- [2] GA Somorjai, "Introduction to Surface Chemistry and Catalysis", Wiley, New York (1994)
- [3] GA Somorjai, Journal of Molecular Catalysis **A107**, 39 (1996)
- [4] FH Streitz, W Mintmire, "Metal/Oxide Interfaces: An Electrostatic-Based Model", Composite Interfaces **2**, 473 (1994)
- [5] AE Carlsson, "Beyond Pair Potentials in Elemental Transition Metals and Semiconductors", Solid State Physics **43**, 1 (1990)
- [6] MS Daw, MI Baskes, "Embedded-Atom Method: Derivation and Application to impurities, surfaces, and other defects", Physical Review **B29**, 6443 (1984)
- [7] SM Foiles, "Calculation of the Surface Segregation of Ni-Cu Alloys with the use of the Embedded-Atom Method", Physical Review **B32**, 7685 (1985)
- [8] MI Baskes, "Modified Embedded-Atom Potentials for Cubic Materials and Impurities", Physical Review **B46**, 2727 (1992)
- [9] L Fast, JM Willis, "Elastic Constants of Hexagonal Transition Metals: Theory", Physical Review **B51**, 17431 (1995)
- [10] EA Seddon, KR Seddon, "The Chemistry of Ruthenium", Elsevier Science, Holland, 1984
- [11] E Clementi, C Roetti, "Roothan-Hartree-Fock Atomic Wavefunctions", Atomic Data and Nuclear Data Tables **14**, 177 (1974)
- [12] S Kirkpatrick, CD Gelatt, MP Vecchi, Science **220**, 671 (1983)

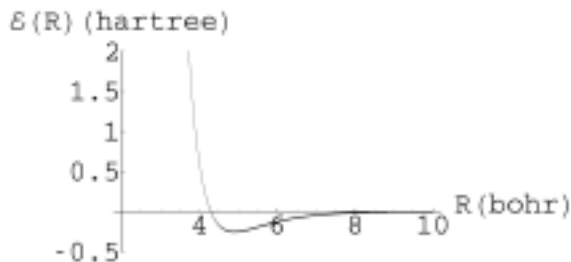


Fig. 4. "Cohesive energy" vs atomic separation. The cohesive energy and near neighbor separation corresponds to the minimum of the curve.

Param.	Fit	Prop.	Calc.	Exper.
$\alpha$	0.9164	$C_{11}$	5.779	5.763
$\beta$	1.037	$C_{12}$	2.145	1.872
$K_o$	197.6	$C_{13}$	1.673	1.673
$a$	288.5	$C_{33}$	5.417	6.405
$b$	65.56	$C_{55}$	1.365	1.891
		$E_{sub}$	0.2485	0.2492

Table 1. Fitting parameters and comparison between calculated and experimental properties.

## APPLICATION: SURFACE ENERGY

Here we calculate the energy necessary to produce a surface from bulk along the "c" direction. We use eq. (1) with the known embedding and repulsive terms for an atom on the surface and then subtract that value from the bulk cohesive energy. This corresponds to the energy necessary to break the interfacial bonds between two semi-infinite slabs of Ru, that is, the surface energy. We obtain a value of 4273 erg/cm<sup>2</sup>, quite in good agreement with typical values for other transition metals [7].

## CONCLUSIONS AND FUTURE WORK

In this work we found the EAM embedding and repulsive functions for ruthenium. We checked the goodness of these functions by calculating the elastic constants and the sublimation energy, and, independently we calculated the energy of surface formation. Future work calls for the introduction of oxygen in the bulk and surface of ruthenium and of electrolyte molecules just outside the metal surface.